Search for Lowest-Energy Nonclassical Fullerenes III: C_{22}

Chad Killblane, Yi Gao, Nan Shao, and Xiao Cheng Zeng*

Department of Chemistry, University of Nebraska-Lincoln, Lincoln, Nebraska 68588

Received: February 23, 2009; Revised Manuscript Received: June 14, 2009

Density functional and second-order Møller−Plesset perturbation (MP2) methods were employed in the investigation of low-lying C_{22} isomers. All cage structures with four-, five-, six-, and seven-membered rings were examined with the monocyclic ring, bowl, and other noncage structures. Cage isomers were first identified via graph theoretical methods, and noncages were identified by basin-hopping methods. Initial isomer screenings were carried out at the PBE/DND level of theory. Low-lying isomers, within 0.6 eV of the predicted lowest-energy isomer, were further evaluated at the PBE1PBE/cc-pVTZ and MP2/cc-pVTZ levels. Our results confirm that the cage structures are more stable than the ring structure and the bowl structure. The lowest-energy structure for C_{22} is predicted to be the C_{22}-1 cage containing one four-membered ring. Anion photoelectron and optical spectra of the six lowest-lying isomers are also computed.

Introduction

Since the discovery of C_{60}, carbon isomers have formed a foundation of nanocluster research.[1,2] Isomers ranging in size from C_{20} to C_{96} have been reported.[3−5] However, only a few of these clusters have been fully examined. The sheer number of isomers for the larger clusters makes doing so intractable. Therefore, it was important to identify the means by which the problem could be truncated. One such scheme is the organization of isomers into two subsets, classical fullerenes and nonclassical fullerenes. Classical fullerenes are composed of pentagons and hexagons, often obeying the isolated pentagon rule (IPR). These isomers are generally more stable than nonclassical fullerenes, those including three-, four-, seven-membered, or larger rings. However, recent theoretical and experimental observations found some exceptions. Fowler et al. employed semiempirical calculations in the examination of fullerenes having one or more four-membered rings.[6] Their results suggest that the inclusion of these smaller rings can lead to energetically competitive isomers. Employing density functional theory (DFT) and X-ray crystallography, Qian et al. found a C_{62} isomer with a four-membered ring.[7] Furthermore, using Hartree−Fock and DFT methods, Díaz-Tendero et al. suggested that the ground state of C_{52}^{2+} adopts a geometry of adjacent pentagons and a four-membered ring.[8] In addition, a non-IPR fullerene derivative, $C_{64}H_4$, was synthesized by introducing methane into the Kratschmer−Huffman method of fullerene production.[9] Higher endofullerenes La@C_{72} and Tb_3N@C_{84} were shown to possess a non-IPR fullerene cage.[10]

The studies mentioned in the preceding paragraph focused on larger fullerenes. When focus is shifted to smaller fullerenes, the prevalence of nonclassical ring sizes is increased. The smallest cluster capable of forming a classical fullerene is C_{20}. Brabec et al. applied quantum molecular dynamics simulations with the Car−Parrinello method to the free energy of C_{20} clusters. Their results show that these isomers favor a transformation from a closed cage structure at low temperatures, to a more open corrannulene-like bowl structure, and ultimately to a ring at high temperatures.[11] Raghavachari et al. investigated C_{20} isomers by both Hartree−Fock and DFT methods; these methods favored the ring and cage, respectively.[12] Applying the CCSD(T)/cc-pVDZ method, An et al. found that the ring isomer is favored at high temperatures and the bowl is favored at low temperatures.[13a] However, when the cluster size is increased from C_{20} to C_{24}, closed cages become the dominant form.[13b] It was generally thought to form the classical fullerene, composed of twelve five-membered rings and two six-membered rings. However, recent DFT calculations[13−16] have shown nonclassical fullerenes to be energetically comparable to the classical isomers.

The work presented here will build upon these previous studies by filling in the gap between these two fullerene sets. It will focus on identifying the ground-state isomer of C_{22}. There have been few previous investigations of the full isomer set, principally because of its lack of a classical fullerene isomer.[16,17] Previous experimental studies have suggested that its ground state is a monocyclic ring.[18] However, theoretical studies have favored cages. In their seminal work, Jones and Seifert identified a series of C_{22} clusters containing both cage and noncage isomers.[16] Therefore, this study aims to predict the true ground state of the C_{22} isomers by an extensive investigation of all possible cage isomers.

In our previous papers (Paper I and Paper II),[19] we reported theoretical predictions of the best candidates for the lowest-energy structures of fullerenes C_{38}−C_{120}. Note that the best candidates for the lowest-energy structures of IPR fullerenes C_{20}−C_{36}[20a,b] and C_{20}−C_{86}[20c,d] have also been systematically studied (except C_{22}). In this article, we present a theoretical study of C_{22}. Previous works have indicated that the addition of nonclassical rings can lead to stable carbon clusters.[7−9,13,16] Therefore, this work will examine all possible C_{22} cage isomers containing four-, five-, six-, and seven-membered rings. It will also compare these cage clusters to the corresponding ring, bowl, and several noncage carbon clusters.

There are three main goals in this study. First, a multifaceted search of these C_{22} clusters will be performed to find a global minimum. Second, all of the clusters that lie within 0.6 eV of the global minimum, as determined by the first-round search, will be further examined by progressively higher levels of theory. Third, simulated anion photoelectron spectra and ultraviolet/visible light absorption spectra as well as NICS values

* Corresponding author. E-mail: xczeng@phase2.unl.edu.

10.1021/jp9016745 CCC: $40.75
Published on Web 07/10/2009

and other properties will be presented and will be used to predict the relative stabilities of these clusters as well as to be compared with future experimental measurements.

Theoretical Method. All cage structures containing four- to seven-membered rings were generated using the Plantri and CaGe programs, of McKay and Brinkman.[21] They generate the initial planar graphs and the translations of those planar graphs into a 3D structures. Each of these initial structures was assigned an integer value during the creation process. This value has been maintained as the clusters identifier, and it does not have an energetic meaning.

Because there is quite a number of planar representation isomers, the basin-hopping global-minimum search method[22] coupled to the self-consistent charge density functional tight binding (SCC-DFTB) model[23] was applied to explore all possible low-lying isomers.[16,20] These two steps generated a total of 318 isomers, of which 218 are closed cages and 100 are not. Each of these isomers was optimized using the DFT method within the generalized gradient approximation (GGA) and with the Perdew−Burke−Ernzerhof (PBE) functional form.[24] The double numerical polarized (DND) basis sets were applied, which are equivalent to 6-31G* basis sets. These calculations were performed with the DMol3 software suite.[25,26]

The isomers within 0.6 eV from the lowest-energy isomer (at the PBE/DND level of theory) were reoptimized using the hybrid PBE1PBE functional with the larger cc-pVTZ basis sets of Dunning and coworkers.[27] In our previous C_{20} study, this functional and basis set combination was found to give excellent agreement with much higher levels of theory.[13] It was used as part of an extensive analysis and was shown to reproduce the ordering of the much higher level CCSD(T)/cc-pVTZ calculations reliably. However, the 0.6 eV cutoff is arbitrary. It was chosen to be large enough (larger than typical error bar of DFT) to ensure a fair sampling of the available clusters but not so large as to make the number intractable.

The optimized structures (at PBE1PBE/cc-pVTZ level) were then subjected to a frequency analysis to ensure that no imaginary frequencies were presented. In addition, single-point energies of the five lowest-lying isomers were computed at the MP2/cc-pVTZ level. The remaining six higher-energy isomers were excluded from the MP2 analyses because there is a large jump in energy between the two sets. These calculations are performed using the Gaussian03 software package.[28]

Several spectral features were also calculated for each of the cage isomers. These features include the anion photoelectron spectra as calculated via the density of states method from the PBE1PBE geometries. Besides the HOMO−LUMO gaps calculated from the orbital eigenvalues of the neutral molecules, the first excited singlets were also calculated from the time-dependent density functional theory (TDDFT). However, as will be shown, the PBE1PBE functional does not represent these features well. Therefore, an extensive functional analysis was carried out on clusters with known experimental quantities, and the PBEPBE functional was found to produce the best results.

Results and Discussions

Relative Stability. The relative energies of the top ten lowest-energy cage isomers at the PBE/DND level are listed in Table 1. Unlike C_{20} and C_{24},[13] C_{22} cannot form a classical fullerene; however, the archetype of a C_{22} classical fullerene would contain twelve pentagons and one hexagon. Note that the terms pentagon, hexagon, and so on should not be taken to have an exact geometric meaning. The terms are simply more convenient then stating the associated ring size. In the total isomer set, four cages (Figure 1) were within the energy-cutoff criteria (0.6 eV). The five noncage isomers along with the bowl (Figure 1) were out of the cutoff range at this level. It should be noted that energy cutoff at the PBE/DND level was applied to the two sets, cage, and noncage, separately, because they were examined

TABLE 1: Cluster Identity, Relative Energy ΔE (electronvolts), and Number and Type of Faces for the Ten Lowest-Lying Cage Isomers Generated by Pantri[a]

cluster	ΔE (eV)	four-membered rings	pentagons	hexagons	heptagons
archetype		0	12	1	0
C_{22}-1[b]	**0.0**	**1**	**10**	**2**	**0**
C_{22}-56	**0.2**	**3**	**6**	**4**	**0**
C_{22}-99	**0.3**	**3**	**6**	**4**	**0**
C_{22}-2[b]	**0.6**	**2**	**8**	**3**	**0**
C_{22}-76	0.7	2	8	3	0
C_{22}-60	0.7	3	6	4	0
C_{22}-98	0.7	3	6	4	0
C_{22}-54	1.0	3	6	4	0
C_{22}-81	1.1	3	7	2	1
C_{22}-61	1.2	3	6	4	0

[a] Four clusters whose energy is within 0.6 eV from the lowest-energy cluster are marked in bold. The energies were calculated using the PBE/DND level of theory. [b] Ref 16.

TABLE 2: Calculated Relative Energies (electronvolts) of the Eleven Isomers Using the PBE1PBE/cc-pVTZ Level of Theory and Relative Energies of the Five Lowest-Lying Isomers at the MP2/cc-pVTZ Level

	PBE1PBE	MP2
isomer	ΔE (eV)	ΔE (eV)
C_{22}-1	0	0
C_{22}-56	0.254	0.210
C_{22}-99	0.458	0.388
C_{22}-ring	0.544	1.283
C_{22}-2	0.68	0.765
C_{22}-bowl	1.559	
C_{22}-nc1	2.786	
C_{22}-nc9	3.667	
C_{22}-nc10	4.44	
C_{22}-nc12	4.065	
C_{22}-nc11	4.518	

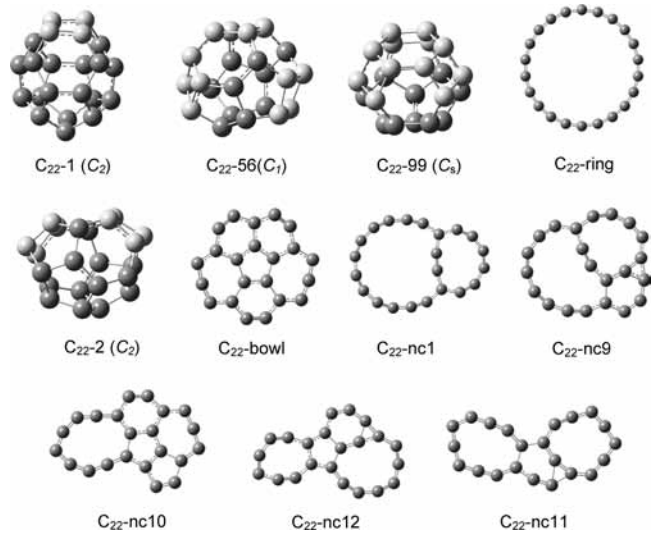

Figure 1. Optimized structures of the eleven isomers, including four cage isomers, one ring, one bowl, and five noncage isomers. The group symmetry of the four cage isomers is given in parentheses. The four-membered rings in the cage isomers are highlighted in pink.

TABLE 3: Calculated HOMO−LUMO Gap (electronvolts), First Excited Singlet, and NICS Value (Using PBEPBE/cc-pVTZ Level of Theory) for the Four Lowest-Lying Cage Isomers

	PBE1PBE/cc-pVTZ		PBEPBE/cc-pVTZ		
isomer	HOMO−LUMO	1st singlet	HOMO−LUMO	1st singlet	NICS
C_{22}-1	2.31	1.19	0.71	0.8	3.68
C_{22}-56	2.48	1.39	0.98	1.12	−31.40
C_{22}-99	2.02	0.90	0.56	0.66	−4.39
C_{22}-2	2.24	1.25	0.72	0.92	−17.03

TABLE 4: Calculated HOMO−LUMO Gaps, First Excited Singlets, and Experimental Gaps for C_{60}, W@Au_{12}[a]

	C_{60}		W@Au_{12}	
Functional	HOMO−LUMO	1st singlet	HOMO−LUMO	1st singlet
B3LYP	2.75	2.09	2.89	1.90
B3PW91	2.76	2.09	3.03	2.03
BP86	1.66	1.68	1.78	1.80
PBEPBE	1.66	1.68	1.81	1.81
PBE1PBE	3.03	2.18	3.33	2.08
experimental	1.73		1.68	

[a] All calculations were carried out with the cc-pVTZ basis sets.

in two separate batch processes. These 11 isomers were then optimized at the PBE1PBE/cc-pVTZ level with the Gaussian03 software suite. The results of these calculations are listed in Table 2, and their structures are shown in Figure 1. In addition, MP2/cc-pVTZ single-point energies have been calculated for each of the five lowest-lying isomers. These results are included in Table 2 as well.

An examination of the ΔE terms in Table 2 shows a large jump of approximately 0.9 eV between the C_{22}-2 and the bowl isomer. Indeed, the ring is the only noncage to be energetically competitive. Therefore, the incorporation of nonclassical rings allows C_{22} to form closed cages. Furthermore, at both the PBE1PBE and MP2 levels, the closed cage isomer C_{22}-1 is confirmed to be the ground state.[16] It is interesting to note that each of the top-three lowest-energy cage isomers contains an odd number of four-membered rings, with one, three, and three, respectively. These results are in line with those of An et al.[13] The inclusion of nonclassical rings therefore can lead to energetically competitive small carbon cages. This seems reasonable because the addition of four-membered rings to the cage always comes at the cost of two five-membered rings. One becomes a four-membered ring and one becomes a six-membered ring.

Chemical Stability and Aromaticity of the Carbon Cage. Table 3 lists the calculated HOMO−LUMO gap, first excited

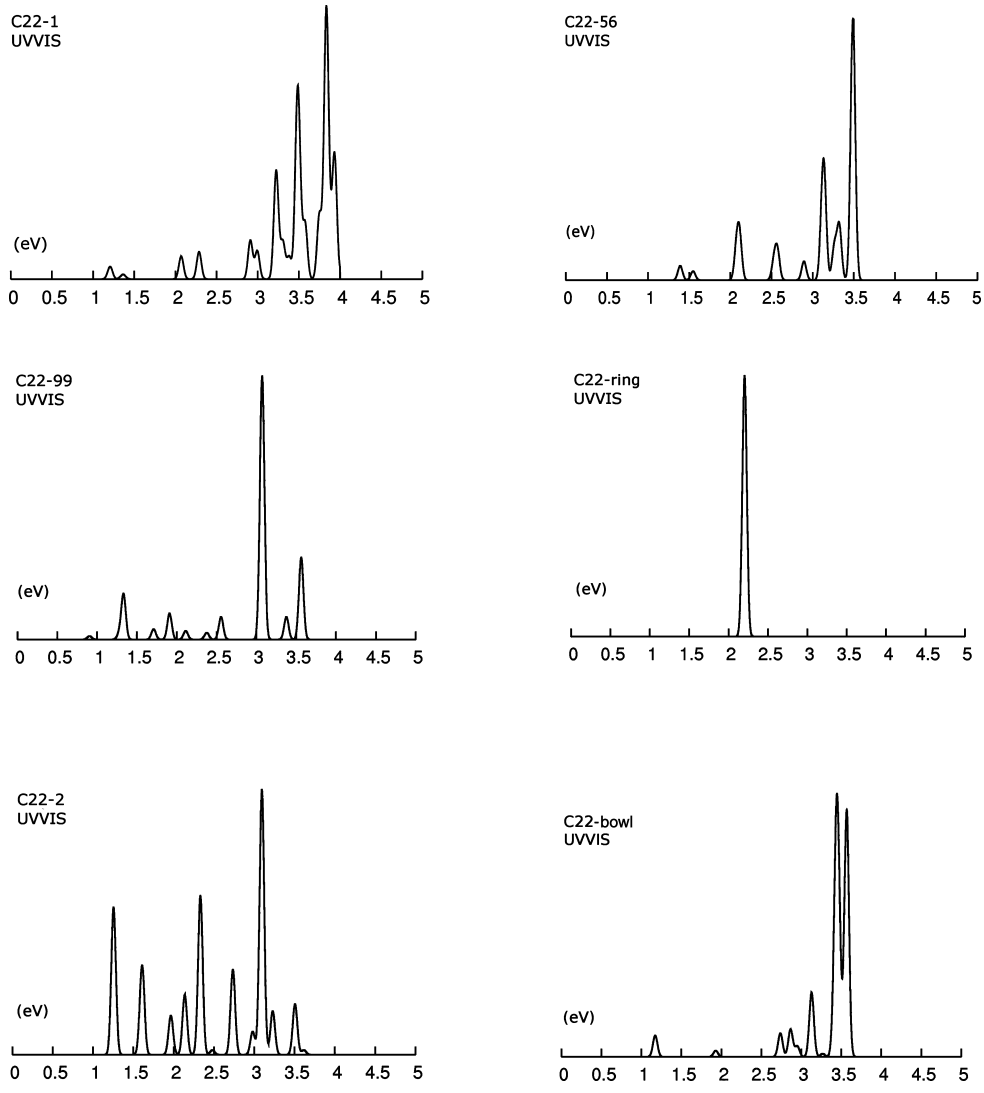

Figure 2. Simulated UV/vis spectra of the six low-lying C_{22} isomers based on the PBE1PBE/cc-pVTZ level of theory.

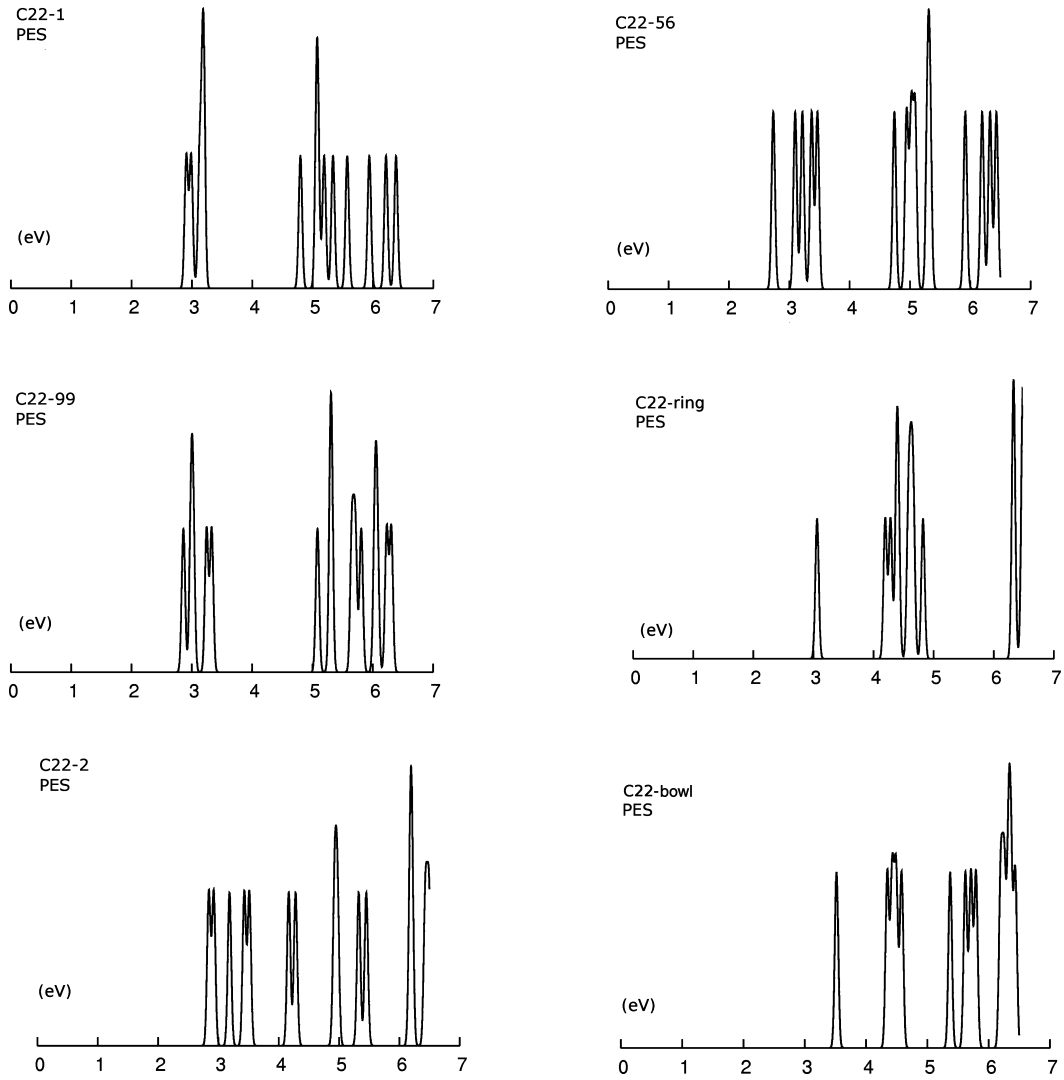

Figure 3. Simulated anion photoelectron spectra of the six low-lying C_{22}^- isomers based on the PBE1PBE/cc-pVTZ level of theory.

singlet, and NICS value for the four lowest-lying cage isomers. Isomers with larger HOMO−LUMO gaps are likely more stable than isomers with smaller HOMO−LUMO gaps.[29] The PBE1PBE/cc-pVTZ results show that the HOMO−LUMO gaps of all cage isomers are between 2.0 to 2.5 eV, similar to the results for C_{20} and C_{24}.[13] However, the first excited singlets of these isomers are between 0.9 and 1.4 eV. The disparity between these two measures is clearly not physically reasonable. The static DFT HOMO−LUMO gap and the first excited singlet given by TDDFT are two measures of the same quantity. TDDFT does include correlation terms between the excited state and electron hole; but these effects tend to increase the value of the singlet with respect to the HOMO−LUMO gap.[30] Furthermore, noting that these increments are on the order of 0.1 to 0.2 eV,[30] it appears that the PBE1PBE/cc-pVTZ level overestimates the value of the HOMO−LUMO gap, which was also indicated by Zhang et al. in recent work.[31] Therefore, it is necessary to use a different functional for the estimation. To this end, we calculated the HOMO−LUMO gap and first excited singlet at several levels of theory for two benchmark clusters, C_{60} and $W@Au_{12}$. These calculations were then compared with the experimental HOMO−LUMO gaps as obtained from their anion photoelectron spectra. These data are collected in Table 4. The data in Table 4 show that the hybrid functionals (PBE1PBE, B3LYP, B3PW91) tend to overestimate the HOMO−LUMO gap values for these benchmark clusters, and the pure density functionals (particularly the PBE functional) give better estimations, which is consistent with previous work.[31]

The nucleus-independent chemical shift (NICS) value, taken at the center of a molecular cage, serves as a measure of spherical aromaticity.[32] Negative NICS values tend to correlate with spherical aromaticity. Therefore, large negative values are an indicator of chemical stability. From an examination of Table 3, there is no clear correlation with the magnitude of gaps and NICS values. Interestingly, the largest value of HOMO−LUMO gap and the largest negative NICS value correspond to the same isomer, although a correlation of two data points does not constitute a generic trend. Furthermore, the ground state candidate C_{22}-1 has a positive NICS value, yet isomer C_{22}-2 has approximately the same value of HOMO−LUMO gap but with a much more negative NICS value. This might be due to the local structure of the two isomers. Referencing Table 1, it can be seen that isomer C_{22}-1 has two hexagons, and isomer C_{22}-2 has three hexagons. In addition, isomer C_{22}-56 has four hexagons and the largest negative NICS value. Therefore, there is a possible trend, namely, increasing the number of hexagons may decrease the NICS value. Therefore, increasing the number of six-membered rings tends to stabilize the cluster.

Given the data, it would seem that isomer C_{22}-56 is the most aromatic. Although NICS values do not always correspond to aromaticity,[33] they do correlate with an overall diatropic current system in the cage. In essence, the large negative NICS values

TABLE 5: Calculated First and Second Vertical Detachment Energies (electronvolts) of Five Lowest-Lying Isomers at the PBE1PBE/cc-pVTZ Level of Theory[a]

isomer	1st VDE (eV)	2nd VDE (eV)
C_{22}-1	2.910	2.986
C_{22}-56	2.736	3.062
C_{22}-99	2.861	3.005
C_{22}-ring	3.061	4.196
C_{22}-2	2.843	2.921

[a] Two values give rise to the position of the first and second peak in the simulated photoelectron spectra shown in Figure 3.

tend to suggest that nonclassical fullerene cages possess a degree of chemical stability and therefore could be synthesized in the laboratory.

Anion Photoelectron Spectra and Optical Spectra. Anion photoelectron spectroscopy (PES) and optical spectra (UV/vis) are powerful experimental tools for the characterization of carbon cluster structures. In Figures 2 and 3, we present the simulated optical spectra of neutral species and PES spectra of anion species for the six low-lying neutral isomers. The UV/vis spectra show a high degree of variability, between the cage and noncage isomers. Overall, the cages have more absorption peaks than the noncage structures. More specifically, C_{22}-1 has two relatively weak absorptions at 1.2 and 1.4 eV. C_{22}-56 has two weak absorption peaks at 1.4 and 1.6 eV, whereas C_{22}-99 has four weak absorption peaks below 2.0 eV. C_{22}-2 has three absorption peaks below 2.0 eV, two strong ones at 1.25 and 1.6 eV, and a weak one at 1.95 eV. The ring isomer has no absorption peak below 2.0 eV, whereas the bowl isomer has two weak absorption peaks below 2.0 eV.

The anion photoelectron spectra are also distinctive. The first vertical detachment energies (VDEs) of the cage structures are below 3.0 eV, and the gap between the first and second VDE for the cage isomers is less than 1 eV (Table 5), which is inconsistent with previous experimental results of ~1.5 eV.[18] However, it is interesting that the VDE of the C_{22}-ring is located near 3.0 eV with a gap between the first and second VDEs close to 1.5 eV; both values fit the previous experiment.[18] This is not an unexpected result because the methodology employed by Yang et al.[18] is known to favor ring formation for small fullerene clusters ($n < 24$). Yet, as shown by Prinzbach et al.,[34] it is possible to synthesize specific metastable clusters by rational design.

Conclusions

All low-lying isomers of C_{22} were systematically studied with the combination of the basin-hopping global optimization and DFT. Our results have shown that among the five lowest-lying isomers, the cage structures take four positions, and only one noncage, that is, the C_{22}-ring, is included at rank 4. All low-lying cage isomers have notably large HOMO−LUMO gaps. However, the lowest-energy isomer, C_{22}-1, has a positive NICS value, whereas the other three lowest-lying cage isomers have negative NICS values. Finally, both optical and anion photoelectron spectra were simulated to be compared with future experiments. In conclusion, the incorporation of four-membered rings allows for the generation of closed cages for C_{22} and the best candidate for the ground state is the closed cage isomer C_{22}-1.

Acknowledgment. This work was supported by NSF (CHE-0427746 and MRSEC DMR-0820521), the Nebraska Research Initiative, and by the University of Nebraska Holland Computing Center.

References and Notes

(1) Kroto, H. W.; Heatch, J. R.; O'Brien, S. C.; Curl, R. F.; Smalley, R. E. *Nature* **1985**, *318*, 162.

(2) Kroto, H. W. *Nature* **1987**, *329*, 529.

(3) Achiba, Y.; Kikuchi, K.; Aihara, Y.; Wakabayashi, T.; Miyake, Y.; Kainosho, M. High Fullerences and Endohedrals. In *The Chemical Physics of Fullerenes 10 (and 5) Years Later: The Far-Reaching Impact of the Discovery of C60*; Andreoni, W., Ed.; Kluwer Academic Publishers: Dordrecht, The Netherlands, 1996; p 139.

(4) Minami, T.; Miyake, Y.; Kikuchi, K.; Achiba, Y. In *The 18th Fullerene General Symposium*; Osawa, E., Ed.; Fullerene Research Association of Japan: Okazaki, Japan, 2000; *1B02*, p 42.

(5) *Carbon Molecules and Materials*; Setton, R., Bernier, P., Lefrant, S., Ed.; Taylor & Francis, Inc.: New York, 2002.

(6) Fowler, P. W.; Heine, T.; Manolopoulos, D. E.; Mitchell, D.; Orlandi, G.; Schmidt, R.; Seifert, G.; Zerbetto, F. *J. Phys. Chem.* **1996**, *100*, 6984.

(7) Qian, W.; Bartberger, M. D.; Pastor, S.; Houk, K. N.; Wilkins, C. L.; Rubin, Y. *J. Am. Chem. Soc.* **2000**, *122*, 8333.

(8) Díaz-Tendero, S.; Martín, F.; Alcamí, M. *ChemPhysChem* **2005**, *6*, 92.

(9) Wang, C. R.; Shi, Z. Q.; Wan, L. J.; Lu, X.; Dunsch, L.; Shu, C. Y.; Tang, Y. L.; Shinohara, H. *J. Am. Chem. Soc.* **2006**, *128*, 6605.

(10) (a) Wakahara, T.; Nikawa, H.; Kikuchi, T.; Nakahodo, T.; Rahman, G. M. A.; Tsuchiya, T.; Maeda, Y.; Akasaka, T.; Yoza, K.; Horn, E.; Yamamoto, K.; Mizorogi, N.; Slanine, Z.; Nagase, S. *J. Am. Chem. Soc.* **2006**, *128*, 14228. (b) Beavers, C. M.; Zuo, T.; Duchamp, J. C.; Harich, K.; Dorn, H. C.; Olmstead, M. M.; Balch, A. L. *J. Am. Chem. Soc.* **2006**, *128*, 11352.

(11) Brabec, C. J.; Anderson, E. B.; Davidson, B. N.; Kajihara, S. A.; Zhang, Q.-M.; Bernholc, J. *Phys. Rev. B* **1992**, *46*, 7326.

(12) Raghavachari, K.; Trucks, G. W.; Head-Gordon, M.; Pople, J. A. *Chem. Phys. Lett.* **1989**, *157*, 479.

(13) (a) An, W.; Gao, Y.; Bulusu, S.; Zeng, X. C. *J. Chem. Phys.* **2005**, *122*, 204109. (b) An, W.; Shao, N.; Bulusu, S.; Zeng, X. C. *J. Chem. Phys.* **2008**, *128*, 084301.

(14) Jensen, F.; Koch, H. *J. Chem. Phys.* **1998**, *108*, 3213.

(15) Feyereisen, M.; Gutowski, M.; Simons, J.; Almlöf, J. *J. Chem. Phys.* **1992**, *96*, 2926.

(16) (a) Jones, R. O.; Seifert, G. *Phys. Rev. Lett.* **1997**, *79*, 443. (b) Jones, R. O. *J. Chem. Phys.* **1999**, *110*, 5189.

(17) (a) Boguslavskiy, A. E.; Ding, H.; Maier, J. P. *J. Chem. Phys.* **2005**, *123*, 034305. (b) Arulmozhiraja, S.; Ohno, T. *J. Chem. Phys.* **2008**, *128*, 114301.

(18) Yang, S.; Taylor, K. J.; Craycraft, M. J.; Conceicao, J.; Pettiette, C. L.; Cheshnovsky, O.; Smalley, R. E. *Chem. Phys. Lett.* **1988**, *144*, 431.

(19) (a) Shao, N.; Gao, Y.; Zeng, X. C. *J. Phys. Chem. C* **2007**, *111*, 17671. (b) Shao, N.; Gao, Y.; Yoo, S.; An, W.; Zeng, X. C. *J. Phys. Chem. A* **2006**, *110*, 7672.

(20) (a) Paulus, B. *Phys. Chem. Chem. Phys.* **2003**, *5*, 3364. (b) Malolepsza, E.; Witek, H. A.; Irle, S. *J. Phys. Chem. A* **2007**, *111*, 6649. (c) Chen, Z. F.; Thiel, W. *Chem. Phys. Lett.* **2003**, *367*, 15. (d) Zheng, G.; Irle, S.; Morokuma, K. *Chem. Phys. Lett.* **2005**, *412*, 210.

(21) (a) Brinkmann, G.; Mckay, B. *Plantri*, version 4.1, 2001. http://cs.anu.edu.au/~bdm/plantri/. (b) Brinkmann, G.; Greenberg, S.; Greenhill, C.; Mckay, B. D.; Thomas, R.; Wollan, P. *Discrete Math.* **2005**, *305*, 33. (c) Brinkmann, G.; Mckay, B. D. *Discrete Math.* **2005**, *301*, 147. (d) Brinkmann, G.; Dress, A. W. M. *Adv. Appl. Math.* **1998**, *21*, 473.

(22) Wales, D. J.; Scheraga, H. A. *Science* **1990**, *285*, 1368.

(23) Elstner, M.; Porezag, D.; Jungnickel, G.; Elsner, J.; Haugk, M.; Frauenheim, T.; Suhai, S.; Seifert, G. *Phys. Rev. B* **1998**, *58*, 7260.

(24) Perdew, J. P.; Burke, K.; Ernzerhof, M. *Phys. Rev. Lett.* **1996**, *77*, 3865.

(25) Delley, B. *J. Chem. Phys.* **1990**, *92*, 508.

(26) Delley, B. *J. Chem. Phys.* **2000**, *113*, 7756.

(27) Woon, D. E.; Dunning, T. H. *J. Chem. Phys.* **1993**, *98*, 1358.

(28) Frisch, M. J.; Trucks, G. W.; Schlegel, H. B.; Scuseria, G. E.; Robb, M. A.; Cheeseman, J. R.; Montgomery, J. A., Jr.; Vreven, T.; Kudin, K. N.; Burant, J. C.; Millam, J. M.; Iyengar, S. S.; Tomasi, J.; Barone, V.; Mennucci, B.; Cossi, M.; Scalmani, G.; Rega, N.; Petersson, G. A.; Nakatsuji, H.; Hada, M.; Ehara, M.; Toyota, K.; Fukuda, R.; Hasegawa, J.; Ishida, M.; Nakajima, T.; Honda, Y.; Kitao, O.; Nakai, H.; Klene, M.; Li, X.; Knox, J. E.; Hratchian, H. P.; Cross, J. B.; Bakken, V.; Adamo, C.; Jaramillo, J.; Gomperts, R.; Stratmann, R. E.; Yazyev, O.; Austin, A. J.; Cammi, R.; Pomelli, C.; Ochterski, J. W.; Ayala, P. Y.; Morokuma, K.; Voth, G. A.; Salvador, P.; Dannenberg, J. J.; Zakrzewski, V. G.; Dapprich, S.; Daniels, A. D.; Strain, M. C.; Farkas, O.; Malick, D. K.; Rabuck, A. D.; Raghavachari, K.; Foresman, J. B.; Ortiz, J. V.; Cui, Q.; Baboul, A. G.; Clifford, S.; Cioslowski, J.; Stefanov, B. B.; Liu, G.; Liashenko, A.; Piskorz, P.; Komaromi, I.; Martin, R. L.; Fox, D. J.; Keith, T.; Al-Laham, M. A.; Peng, C. Y.; Nanayakkara, A.; Challacombe, M.; Gill, P. M. W.; Johnson,

B.; Chen, W.; Wong, M. W.; Gonzalez, C.; Pople, J. A. *Gaussian 03*, revision C.02; Gaussian, Inc.: Wallingford, CT, 2004.

(29) (a) Manolopoulos, D. E.; May, J. C.; Down, S. E. *Chem. Phys. Lett.* **1991**, *181*, 105. (b) Hess, B. A., Jr.; Schaad, L. J. *J. Am. Chem. Soc.* **1971**, *93*, 2413. (c) Haddon, R. C.; Fukunaga, T. *Tetrahedron Lett.* **1980**, *21*, 1191. (d) Aihara, J. *J. Phys. Chem. A* **1999**, *103*, 7487.

(30) Killblane, C.; Gao, Y.; Zeng, X. C. *J. Comput. Theor. Nanosci.* **2009**, *6*, 359.

(31) Zhang, G.; Musgrave, C. B. *J. Phys. Chem. A* **2007**, *111*, 1554.

(32) von Rague-Schleyer, P. v. R.; Maerker, C.; Dransfeld, A.; Jiao, H.; van Eikema Hommes, N. J. R. *J. Am. Chem. Soc.* **1996**, *118*, 6317.

(33) Cyrañski, M. K. *Chem. Rev.* **2005**, *105*, 3773.

(34) Prinzbach, H.; Weiler, A.; Landenberger, P.; Wahl, F.; Wörth, J.; Scott, L. T.; Gelmont, M.; Olevano, D.; Issendorff, B. V. *Nature* **2000**, *407*, 60.

JP9016745